Composites Part C: Open Access 11 (2023) 100362

Contents lists available at ScienceDirect

Composites Part C: Open Access

journal homepage: www.elsevier.com/locate/composites-part-c-open-access

Composite material identification as micropolar continua via an optimization approach

Marco Colatosti [a], Biagio Carboni [a], Nicholas Fantuzzi [b,*], Patrizia Trovalusci [a]

[a] DISG Department, Sapienza University of Rome, Via A. Gramsci 53, 00197, Rome, Italy
[b] DICAM Department, University of Bologna, Viale del Risorgimento 2, 40136, Bologna, Italy

ARTICLE INFO

Keywords:
Composite materials
Multiscale procedures
Micropolar continua
Dynamics
Material identification

ABSTRACT

A strategy based on material homogenization and heuristic optimization for the structural identification of composite materials is proposed. The objective is the identification of the constitutive properties of a micropolar continuum model employed to describe the mechanical behaviour of a composite material made of rigid blocks and thin elastic interfaces. The micropolar theory (Cosserat) has been proved to be capable of properly accounting for the particles arrangements as well as their size and orientation. The constitutive parameters of the composite materials, characterized by different textures and dimensions of the rigid blocks, are identified through a homogenization procedure. Thus, the identification is repeated exploiting the static or modal response of the composite materials and using the Differential Evolution algorithm. The benchmark structures assumed as target are represented by discrete models implemented in ABAQUS where the blocks and the elastic interfaces are modelled by rigid bodies and elastic interfaces, respectively. The obtained results show that proposed strategies provide accurate results paving the way to the experimental validation and in field applications.

1. Introduction

The study of composite materials such as ceramic and metal composites, poly-crystals, but also of classical materials such as masonry structures and porous rocks is a non trivial task. The reason is due to the presence of discontinuities and heterogeneities in the internal microstructure of these materials: microcracks, voids, inclusions are important because they influence the macroscopic behaviour of this kind of media.

A composite material made of rigid blocks and elastic interfaces is a heterogeneous material and it may be studied using a micromechanical approach, that provides an accurate evaluation of the material response. However, the drawback is the high computational costs deriving from the many degrees of freedom of the model [1]. A different approach is the macromechanical modelling of the material, which assumes the composite material as a continuum model, whose mechanical properties are derived from a homogenization process. In this way, the individual phases of the inner microstructure are not distinguished. This involve less computational effort than a micromechanical modelling. The referenced continuous model, on the other hand, must be suitable to provide the fundamental mechanical properties of the material.

For these reasons, to account for the microscopic effect on the macroscopic mechanical behaviour, a non-local description is necessary. In the presence of internal length parameters and dispersion characteristics [2–4], continuum theories have a non-local nature and Cosserat or micropolar model, that can be considered as 'implicitly non-local' [5,6], has been used to explain materials made up of rigid particles that interact through elastic surfaces at various scale levels [7–13]. In the micropolar theory additional degrees of freedom are included: the rotation of the particles, the microrotation, is introduced. It is useful to distinguish between the microrotation and the macrorotation, the classical local rigid rotation, defined as the skew-symmetric part of the gradient of displacement. The effects of these rotations, on composite material, such as masonry materials, have been already highlighted [14,15]. Moreover, many various types of composite materials have been modelled as micropolar continua, like masonry structures [16–26], as well as ceramic materials [27,28], granular and geo-materials [29–31] and heterogeneous materials in general [32–35].

It is important to emphasize the wide applicability of multiscale homogenization both for periodic [36,37] and random composites [38–40]. Normally, the Cauchy continuum is not always adequately

* Corresponding author.
E-mail addresses: marco.colatosti@uniroma1.it (M. Colatosti), biagio.carboni@uniroma1.it (B. Carboni), nicholas.fantuzzi@unibo.it (N. Fantuzzi), patrizia.trovalusci@uniroma1.it (P. Trovalusci).

https://doi.org/10.1016/j.jcomc.2023.100362
Received 25 February 2023; Received in revised form 10 May 2023; Accepted 15 May 2023
Available online 18 May 2023

to catch the mechanical response of a composite material, instead, a micropolar model is able to provide more satisfactory results [20,41,42].

In static and dynamic analyses [12,43], it has been shown that, unlike the classical model, a micropolar continuum is capable of recreating the dynamic behaviour of a (discrete) micromechanical system with significant fidelity. As a result, there is interest in establishing a methodology for estimating the constitutive parameters of a composite material as a micropolar continuum, which is a challenging task due to the presence of features that account for the internal dimensions of the microstructure.

The Differential Evolution Algorithm (DE) is a genetic algorithm [44] and it can be a suitable tool for estimating the micropolar constants of a material exploiting the results obtained from static or dynamic analyses. The algorithm has been already applied in various structural problems [45–48], such as systems identification [49,50], health monitoring [51,52] and optimization [53].

In this paper, 2D composite materials with two different textures and two different internal length scales are investigated. A continuum model, for simulating the static and dynamical behaviours of the materials, is implemented while a discrete model, realized in ABAQUS and constituted by rigid particles and linear elastic interfaces, is assumed as the benchmark. The equivalent constitutive matrices of the relative micropolar continuum are estimated using a homogenization technique. Thus, the identification is performed again exploiting the static response for a given load condition or the eigenfrequencies of the discrete model trough an optimization procedure based on the Differential Evolution (DE) algorithm. In particular, the constitutive parameters are identified by minimizing the difference between the displacement field or the eigenfrequencies of the micromechanical model with respect to the reference values provided by discrete model. The obtained results show that very accurate identifications can be achieved with both approaches and the proposed strategies seem to be promising for real applications.

The paper is organized as follows. A brief introduction to micropolar theory is provided, then, the identification of the material constants trough the homogenization technique and the DE algorithm is illustrated. Finally, the results are compared and discussed and the conclusions are formulated.

2. Micropolar continuum

In the 2D dimensional case, the micropolar theory provides three degrees of freedom: two translational displacements u_1, u_2 and the micro-rotation ω. Therefore, the displacement vector is defined as: $\boldsymbol{u}^\top = \begin{bmatrix} u_1 & u_2 & \omega \end{bmatrix}$. At this point, the strain vector is $\boldsymbol{\varepsilon}^\top = \begin{bmatrix} \varepsilon_{11} & \varepsilon_{22} & \varepsilon_{12} & \varepsilon_{21} & \kappa_1 & \kappa_2 \end{bmatrix}$: the terms ε_{ij} are the normal and tangential strain components, where ε_{12} and ε_{21} are different, and two new components arise with respect to the classic model, the microcurvatures κ_1 and κ_2. The stress field is represented by the vector $\boldsymbol{\sigma}^\top = \begin{bmatrix} \sigma_{11} & \sigma_{22} & \sigma_{12} & \sigma_{21} & \mu_1 & \mu_2 \end{bmatrix}$: the terms σ_{12}, σ_{21} are not equal, and the terms μ_1, μ_2 denote the microcouples.

In elasticity, the strain and stress fields are linked trough the constitutive matrix $\mathbf{C}$. Thus, the micropolar anisotropic constitutive equation has the form:

$$\boldsymbol{\sigma} = \mathbf{C}\,\boldsymbol{\varepsilon} \tag{1}$$

where:

$$\mathbf{C} = \begin{bmatrix} A_{1111} & A_{1122} & A_{1112} & A_{1121} & B_{111} & B_{112} \\ & A_{2222} & A_{2212} & A_{2221} & B_{221} & B_{222} \\ & & A_{1212} & A_{1221} & B_{121} & B_{122} \\ & & & A_{2121} & B_{211} & B_{212} \\ & & & & D_{11} & D_{12} \\ sym & & & & & D_{22} \end{bmatrix} = \begin{bmatrix} \mathbf{A} & \mathbf{B} \\ \mathbf{B}^\top & \mathbf{D} \end{bmatrix} \tag{2}$$

For hyperelastic materials, the constitutive matrix is symmetric ($\mathbf{C} \in Sym$), and in particular, $A_{ijhk} = A_{hkij}$; $B_{ijh} = B_{hij}$; $D_{ij} = D_{ji}$ [54].

In a 2D framework, two microstructured materials are considered and a reference block of dimensions 0.05×0.25 is assumed, where 0.05 is the height and 0.25 the width of the block. In order to take into account the internal length scale of the material, a scale factor s is considered and it is defined as a pure scalar value that provides a homothetic transformation of the microstructure. A scale factor $s = 1$ implies that the considered microstructure of the composite material has the blocks with dimensions equal to the reference block. On the other hand, a scale factor equal to $s = 0.5$, means that the block dimensions are all multiplied for a 0.5 factor, therefore a homothetic transformation of the blocks is applied. The dilatancy effect is not taken into account [15,55,56]. The two different textures in question are reported in Fig. 1: for the texture 1 we have interlocking among the blocks, instead for the texture 2, there is no interlocking. In the same figure, the representative volume elements (RVEs) necessaries for the homogenization procedure are depicted. The RVE is defined as the elementary volume element consisting of the minimum number of elements sufficient to correctly catch the mechanical behaviour of the material. It is also crucial that it maintains the material symmetry. Here, the adopted homogenization technique, based on the Cauchy-Born rule, is founded on an equivalence energy criterion between a complex lattice model and a continuum model whereas a kinematic correspondence map is assumed. Details about these aspects can be found in [2,57,58].

3. The differential evolution algorithm for material identification

The estimation of the constitutive parameters for the micropolar continuum necessitates special care due to the internal scale dependency of the model. The elastic parameters for a Cauchy continuum may be evaluated using traditional material characterization tests as well as for the Cosserat model. However, in a number of actual applications, the determination of the micropolar elastic properties based on direct measurements on the examined structure may be required. The Differential Evolution (DE) is a genetic algorithm that belongs to the class of the heuristic optimization techniques. It is used in several applications for optimization and identification because of its adaptability to different objective functions. Here, the static and modal responses of a 2D rectangular panel, clamped at the bottom, are considered. For the first case, the goal is to minimize the mean square error (MSE) between the displacement fields induced by an external load computed with the micropolar model and those provided by the reference discrete model (Eq. (3)). In the second case, the mean square error function to minimize is represented by the difference between the natural vibration frequencies of the panel computed with the micropolar model and those obtained with the reference discrete model (Eq. (4)).

The procedure begins by defining an initial population that includes the parameters to be identified in defined searching spaces. The population is represented by a $(m \times n)$ matrix, where m denotes the number of parameters and n denotes the number of discrete values defined in each assumed interval according to appropriate probability distributions. The initial population is improved with regard to the objective function yielding a new enhanced population by performing the operations of mutation, crossover, and selection. The method is iterated until a certain accuracy of the objective function is attained and the best vector of the last population is assumed as optimal solution. Further details about the algorithm can be found in [44,59].

The parameters of the constitutive matrix $\mathbf{C}$ which have been identified are $A_{1111}, A_{2222}, A_{1212}, A_{2121}, D_{11}, D_{22}$ while the remaining parameters have been assumed according to homogenization-based procedure. Each parameter is discretized with a number of 50 values normally distributed on its research space obtaining an initial population of size 6×50. The coefficient for the differential perturbation is assumed equal to 0.9 and the crossover operation is performed according to a uniform probability distribution in the range (0–1) with discriminant value 0.5 [59].

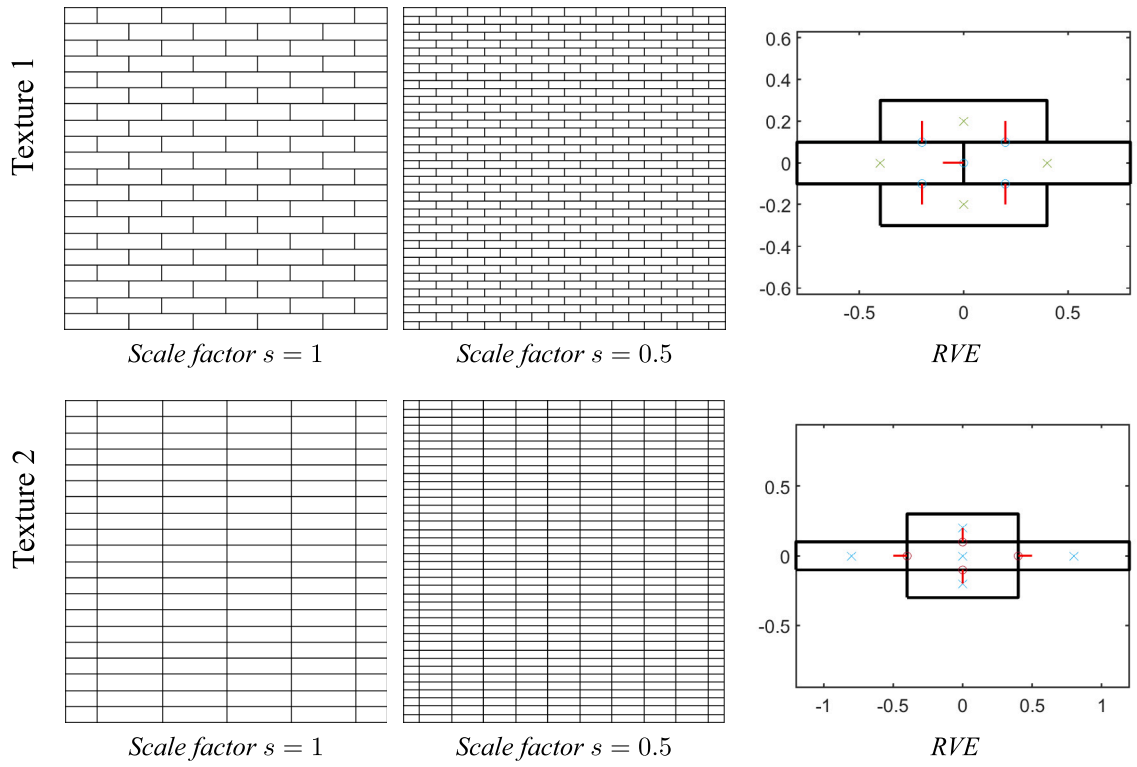

Fig. 1. Rectangular microstructures and respective RVEs of texture with interlocking and texture with no interlocking.

For the static case, the objective function to minimize is the mean square error (MSE) defined as:

$$MSE_s = \frac{100}{Ne_f}\sum_{k=1}^{N}[\boldsymbol{u}_k(\boldsymbol{p}) - \overline{\boldsymbol{u}}_k]^2 \tag{3}$$

where $\boldsymbol{u}_k(\boldsymbol{p})$ represents the displacement vector obtained by the solution of the continuum FEM problem; $\boldsymbol{p}$ indicates the vector collecting the tentative constitutive parameters and $\overline{\boldsymbol{u}}_k$ is the displacement fields obtained with the discrete FEM model. The term e_f indicates the variance of the target displacements $\overline{\boldsymbol{u}}_k$ in the N nodes of the FEM mesh.

In the dynamic case, the objective function is defined as:

$$MSE_d = \frac{100}{Ne_f}\sum_{k=1}^{N}[f_k(\boldsymbol{p}) - \overline{f}_k]^2 \tag{4}$$

where $f_k(\boldsymbol{p})$, with $k = 1, \dots, \mathrm{N}$, represents the lowest N natural frequencies of the continuum micropolar model, $\boldsymbol{p}$ indicates the vector collecting the tentative constitutive parameters and $\overline{f}_k$ is the kth natural frequency obtained with the discrete FEM model. The term e_f indicates the variance of the N (set to 10) lowest target frequencies ($\overline{f}_k$ with $k = 1, \dots, \mathrm{N}$).

4. Numerical simulations

The panel is clamped at the bottom and it is subjected to a horizontal load, distributed on a footprint of width $a = Ly/4$ starting from the top left edge and whose resultant is equal to a force $F = 1 \cdot 10^5$ N. For the same panel with the same boundary conditions, the natural frequencies have been computed. In the next sections, the static and the dynamic analyses of the micromechanical models are reported. The discrete systems are modelled with the help of the commercial code ABAQUS, meanwhile the code of the Cosserat model is an in-house based on the Finite Element Method (FEM) and it is implemented in MATLAB environment [60]. For the texture 1, the panel has dimensions $L_x = 3.2$ and $L_y = 2.4$, while, for the texture 2, the dimensions are $L_x = 2$ and $L_y = 2.4$ and, for simplicity, the thickness of the panel is assumed unitary. The material density is assumed equal to $\rho = 1800$ for both panels.

4.0.1. *Texture 1 — scale factor* $s = 1$

The displacement fields provided by the discrete FEM model are reported in Fig. 2: the displacement vectors represent the target in the objective function expressed by Eq. (3) for the identification of the micropolar constants.

The lowest ten natural frequencies obtained with the discrete model are reported in Table 1. These values represent the target in the objective function expressed by Eq. (4) for the identification of the micropolar constants based on the DE algorithm.

The parameters of the constitutive matrices, for the case of texture with interlocking and internal scale size $s = 1$, obtained via the homogenization approaches and via the DE algorithm, are shown in Table 2. For both static and dynamic case, the elastic constants are identified performing 500 iterations with DE algorithm.

The constitutive matrix of the continuum model is centrosymmetric and orthotropic (see Eq. (2)). Only the submatrix $\mathbf{D}$ takes into account the internal scale of the microstructure. Because of the central symmetry and due to the absence of dilatancy effect in the discrete original model, the submatrix $\mathbf{B} = \mathbf{0}$ and there is no coupling between normal and shear stresses/strains with curvatures/microcouples. Moreover, no Poisson effect is present.

As shown in Table 2, the elastic constant A_{1111} presents similar values in the case of the identification procedures based on DE while the lowest value is related to the homogenization technique. The values A_{2222} are very close for all three cases as well as for the values of A_{1212}. As regards the value of A_{2121}, the lowest value is obtained trough the DE-based static identification. Finally, the micropolar terms D_{11} is exactly the same for the DE-based identifications while there is an one order of magnitude of difference with respect to the homogenization. The values of D_{22} are different for the three cases.

The MSEs computed according to the displacement fields with respect to the discrete FEM model (i.e. Eq. (3)) are $1.55 \cdot 10^{-1}$ and

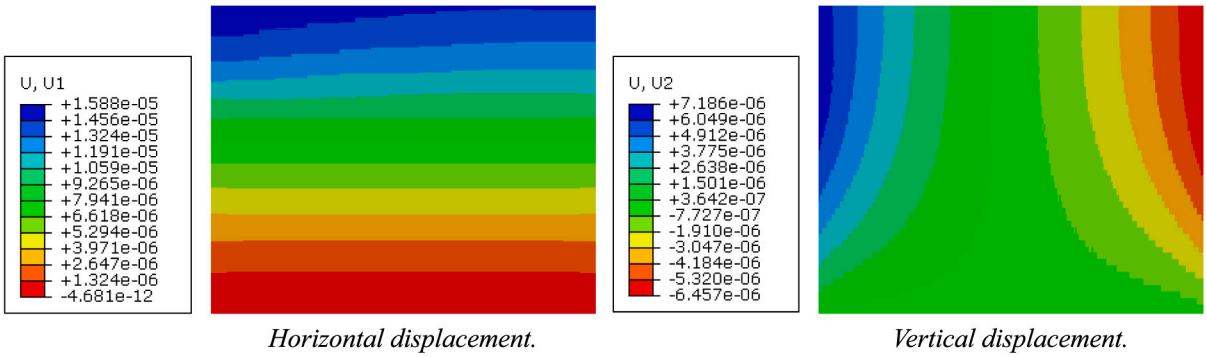

Fig. 2. Displacement fields provided by the discrete FEM model for the texture with interlocking and scale factor $s = 1$.

Table 1
Natural frequencies provided by the discrete FEM model for the texture 1 and scale factor $s = 1$.

Mode	1	2	3	4	5	6	7	8	9	10
Freq. [Hz]	176.3	387.4	431.7	735.5	802.8	1036.4	1163.9	1178.7	1291.3	1328.4

Table 2
Elastic constants for the texture 1 scale $s = 1$.

Constants	Elastic constants		
	Homogenization	Static ID	Dynamic ID
A_{1111} [Pa]	127600000000	215604940688	255200000000
A_{2222} [Pa]	25000000000	24913323520	24943328701
A_{1212} [Pa]	10420000000	10626106611	20220248394
A_{2121} [Pa]	182290000000	122340403964	18229000000
D_{11} [Pa]	940000000	94000000	94000000
D_{22} [Pa]	140000000	14000000	95219108

$9.34 \cdot 10^{-4}$ for the homogenization procedure and the DE-based static identification, respectively. Fig. 3 shows the horizontal and vertical displacement fields evaluated with the micropolar continuum model using the constitutive parameters provided by the homogenization procedure and the DE algorithm according to the static and modal responses of the composite panel. In all three cases, the displacement fields have a good correspondence with the discrete system.

Table 3 reports the comparison of the lowest 10 natural frequencies obtained with the discrete model and the Cosserat models, considering the three constitutive matrices provided by the three different approaches. The percent variations of each natural frequency with respect to the reference values provided by the discrete FEM model are also shown. The MSEs considering the natural frequencies (see Eq. (4)) are $7.69 \cdot 10^{-1}$ and $1.33 \cdot 10^{-3}$ for the homogenization procedure and the DE-based dynamic identification, respectively. As expected, a lower error is achieved with the DE identification based on the modal response according to the fact that the frequency differences are specifically minimized. However, a good accuracy is achieved for all the cases.

4.1. Texture 1 — scale factor $s = 0.5$

The displacement fields provided by the discrete FEM model for the texture 1 with a internal scale $s = 0.5$ are depicted in Fig. 4 while the natural frequencies are reported in Table 4.

The constitutive matrices obtained via the homogenization and DE-based identifications for the case of blocks with interlocking and scale size $s = 0.5$ are reported in Table 5.

The submatrix **A** not depends on the internal length of the microstructure, for this reason the same values obtained for the scale equal to 1 have been found (see Tables 2 and 5). The internal size is taken into account by the submatrix **D**. We can observe that respect to case with the scale equal to 1, the terms D_{11} has the same order of magnitude for the homogenization and the identification performed with the DE algorithm. Moreover, the values of the elastic constant D_{22} provided through the homogenization and through the DE identification based on the static response are similar. The appreciable decrease of the values contained in the submatrix **D**, by means of the homogenization procedure with respect to the case $s = 1$, is a further evidence of the need for a theory that accounts for the scale effect.

The MSEs computed according the displacement fields (see Eq. (3)) are $3.02 \cdot 10^{-2}$ and $4.75 \cdot 10^{-4}$ for the homogenization procedure and the static identification using the DE algorithm, respectively. The errors are for both cases lower than those obtained for the scale $s = 1$. This result is expected considering that the material internal length decreases. Fig. 5 shows the horizontal and vertical displacement fields evaluated with the micropolar continuum model using the constitutive parameters provided by the homogenization procedure and the DE algorithm according to the static and modal responses of the composite panel.

The comparison between the lowest 10 natural frequencies provided by the discrete FEM model and the Cosserat model, whose constitutive matrices have been computed through the homogenization procedure and the DE-based identifications, is shown in Table 6. The MSEs according to Eq. (3) are $1.57 \cdot 10^{-1}$ and $2.02 \cdot 10^{-3}$ for the homogenization procedure and the DE identification based on the dynamic response, respectively. Also in this case, the MSEs decrease for both cases with respect to the results obtained for the scale $s = 1$.

4.1.1. Texture 2 - scale factor s=1

The displacement fields due to the horizontal load employing the discrete FEM model are reported in Fig. 6 while Table 7 shows the natural frequencies.

The constitutive matrices obtained via the homogenization procedure and the identifications based on the DE algorithm for the texture 2 (no interlocking) and scale size $s = 1$ are reported in Table 8.

Differently from the texture 1, the elastic constant A_{1111} presents two close values obtained through the homogenization procedure and the DE identification based on the static response. The values of the term A_{2222} are similar, while the values of A_{1212}, A_{2121}, D_{11} and D_{22} are different for all three approaches.

Fig. 7 shows the displacement fields evaluated with the micropolar continuum model using the constitutive parameters provided by the homogenization procedure and the DE algorithm according to the static and modal responses of the composite panel. The MSEs are $1.02 \cdot 10^{-1}$ and $1.50 \cdot 10^{-3}$ for the homogenization and identification via DE algorithm based on the static response, respectively.

The comparison between the natural frequencies computed with the micromechanical model and the reference discrete model are reported

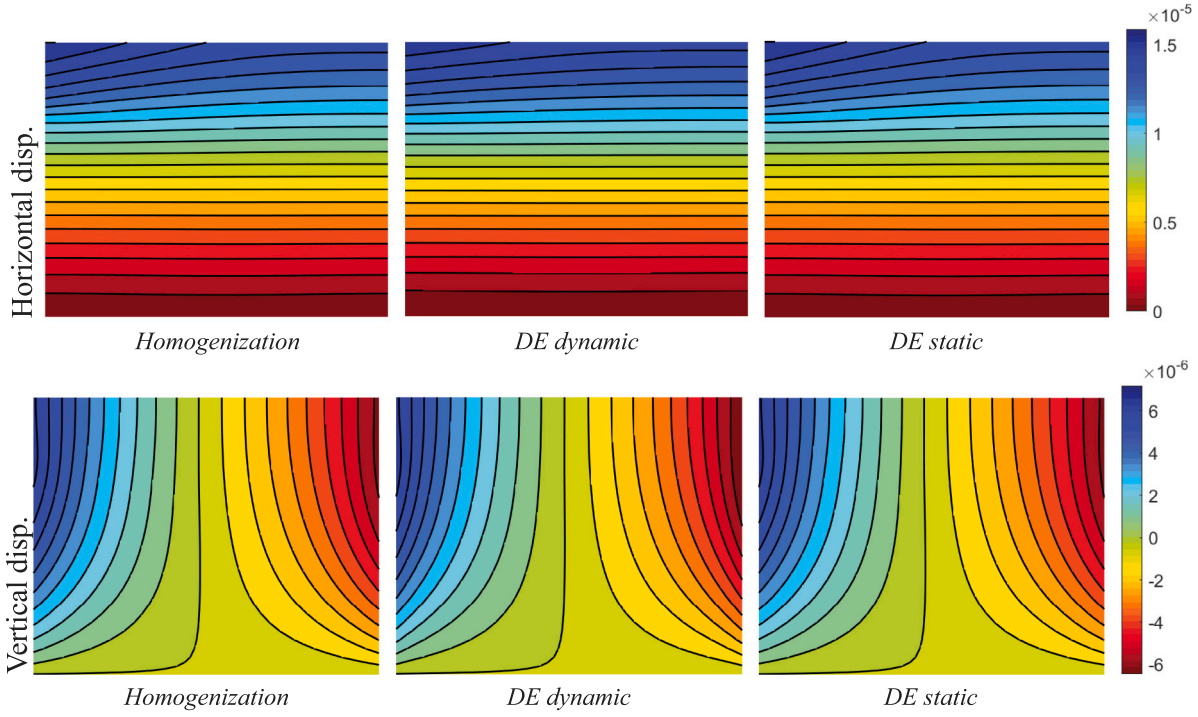

Fig. 3. Displacement fields of the Cosserat continua for the texture 1 with interlocking and scale factor $s = 1$.

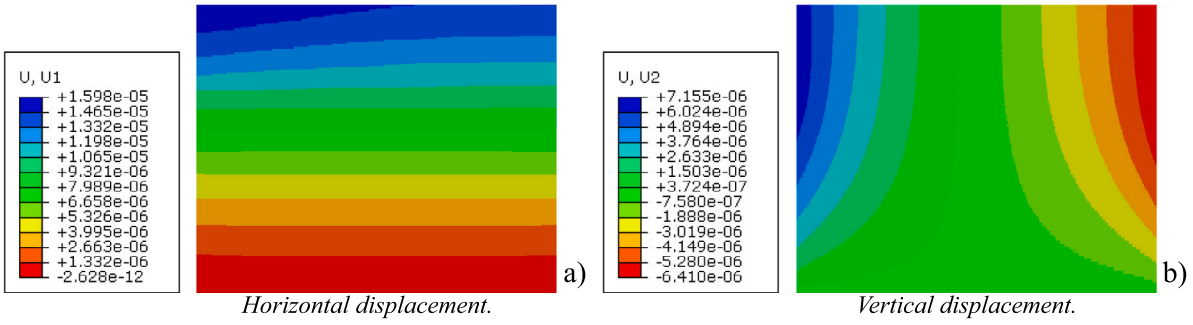

Fig. 4. Displacement fields of the Cosserat continua for the texture 1 with interlocking and scale factor $s = 0.5$.

Table 3
Natural frequencies for the texture 1 and scale factor $s = 1$.

Mode	Frequencies [Hz]						
	Discrete	Homogenization	Error [%]	Dynamic ID	Error [%]	Static ID	Error [%]
1	176.3	180.8	−2.57	178.9	−1.47	180.8	−2.57
2	387.4	388.2	−0.21	387.8	−0.11	388.2	−0.21
3	431.7	435.1	−0.77	434.5	−0.64	435.1	−0.77
4	735.5	753.9	−2.50	734.8	0.09	753.9	−2.50
5	802.8	817.0	−1.77	801.1	0.20	817.0	−1.77
6	1036.4	1053.7	−1.67	1036.5	0.0	1053.7	−1.66
7	1163.9	1165.7	−0.15	1164.3	−0.03	1165.7	−0.15
8	1178.7	1285.7	−9.1	1180.3	−0.13	1285.7	−9.08
9	1291.3	1292.2	−0.07	1290.3	0.075	1232.2	4.58
10	1328.4	1354.7	−1.98	1327.3	0.08	1354.7	−1.98

Table 4
Natural frequencies provided by the discrete FEM model for the texture 1 and scale factor $s = 0.5$.

Mode	1	2	3	4	5	6	7	8	9	10
Freq. [Hz]	180.3	383.8	428.9	737.3	798.6	1038.5	1163.0	1187.4	1293.9	1325.8

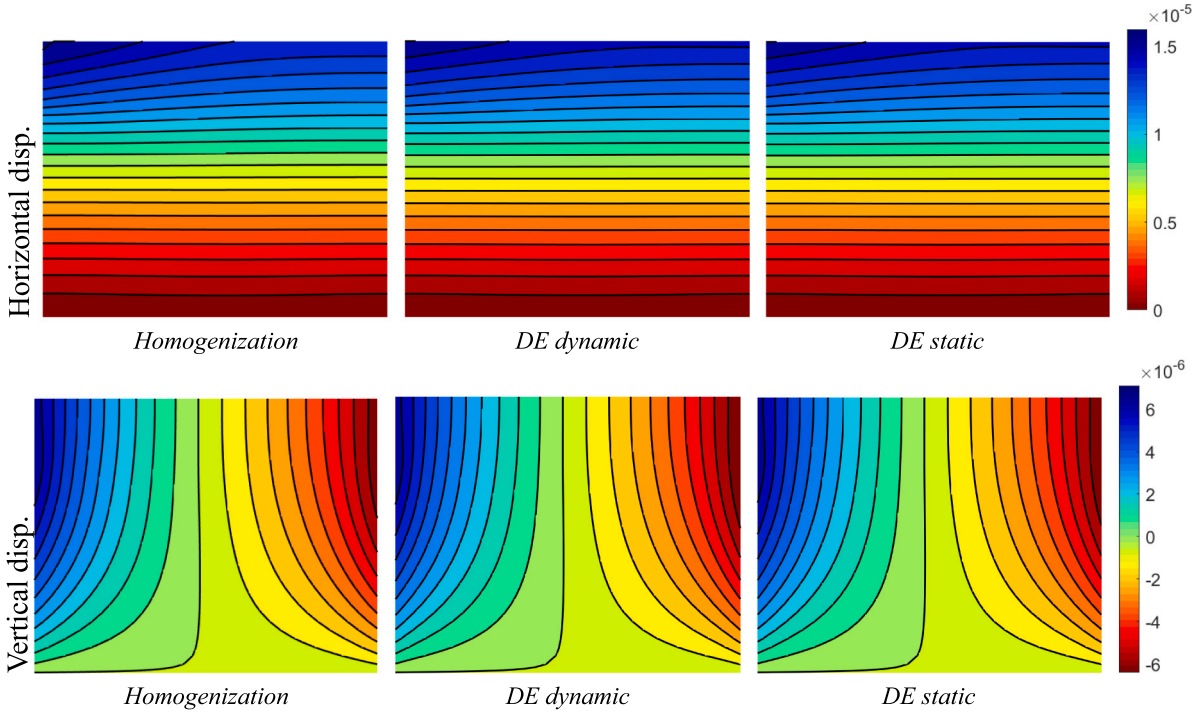

Fig. 5. Displacement fields of the Cosserat continua for the texture 1 with interlocking and scale factor $s = 0.5$.

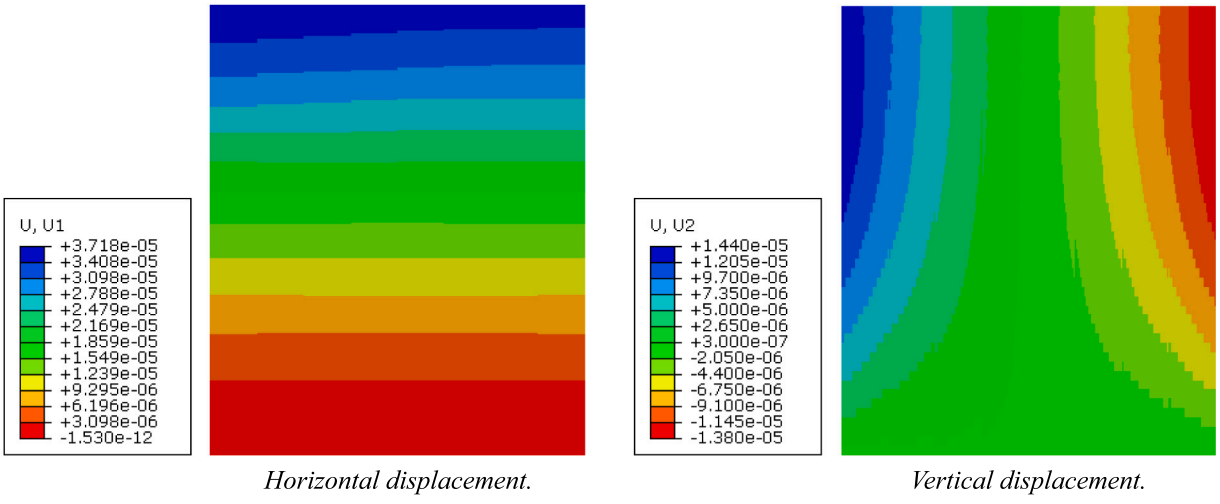

Fig. 6. Displacement fields of the Cosserat continua for the texture 2 with no interlocking and scale factor s = 1.

Table 5
Elastic constants for the texture 1, scale $s = 0.5$.

Constants	Elastic constants		
	Homogenization	Static ID	Dynamic ID
A_{1111} [Pa]	127600000000	196117732316	204098165389
A_{2222} [Pa]	25000000000	24923994248	24840986104
A_{1212} [Pa]	10420000000	10649230684	10542599120
A_{2121} [Pa]	182290000000	119204399689	141338068988
D_{11} [Pa]	240000000	111164609	25952956
D_{22} [Pa]	40000000	40180131	47552061

in Table 9. We can observe a good accuracy in the identification of the natural frequencies for all procedures. Moreover, the DE algorithm provide a very precise identification of the higher structural frequencies. The MSEs are $1.52 \cdot 10^{-1}$ and $1.67 \cdot 10^{-3}$ for the homogenization and the DE identification based on the modal response, respectively.

4.2. Texture 2 - scale factor s=0.5

The horizontal and vertical displacement fields computed with the discrete FEM for the texture 1 with an internal scale $s = 0.5$ are shown in Fig. 8 while the natural frequencies are reported in Table 10.

The constitutive matrices obtained via the homogenization procedure and the identification based on the DE algorithm for the case of blocks with no interlocking and scale factor $s = 0.5$ are shown in Table 11. With respect to the case with $s = 1$, the scale reduction involves a decrease of the elastic constant A_{1111} for the modal-based identification and becomes closer to the values identified via homogenization and static response. The micropolar term D_{11} is the same for both identifications based on the static and dynamic response, while the constants D_{22} assumes different value between the three approaches.

The displacement fields provided by static analyses of the micropolar continuum and by using the elastic constants obtained through

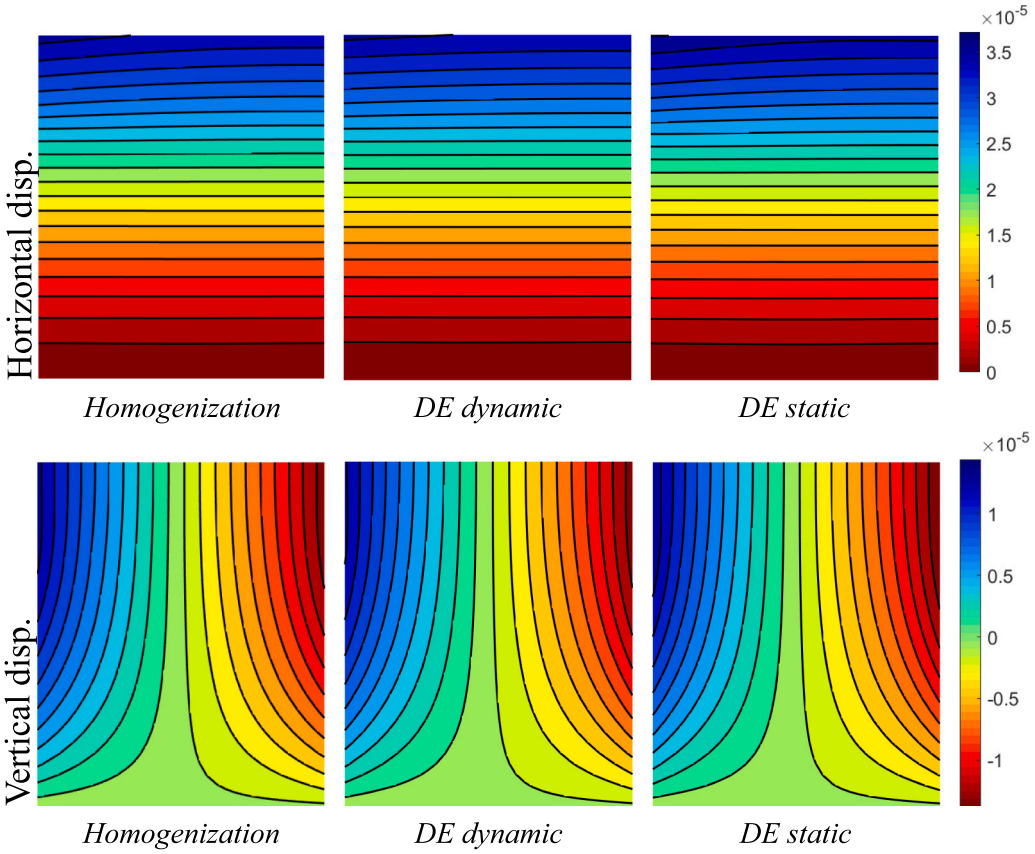

Fig. 7. Displacement fields of the Cosserat continua for the texture 2 with no interlocking and scale factor $s = 1$.

Table 6
Natural frequencies for the texture 1 and scale factor $s = 0.5$.

Mode	Frequencies [Hz]						
	Discrete	Homogenization	Error [%]	Dynamic ID	Error [%]	Static ID	Error [%]
1	180.3	179.4	0.79	178.4	1.35	178.6	1.23
2	383.8	388.2	−1.13	387.0	−0.82	387.7	−1.00
3	428.9	434.6	−1.31	432.5	−0.83	433.1	−0.96
4	737.3	742.1	−0.64	736.0	0.17	737.4	0.00
5	798.6	792.8	0.72	799.7	−0.13	805.1	−0.82
6	1038.5	1046.0	−0.72	1039.4	−0.08	1042.0	−0.33
7	1163.0	1165.7	−0.23	1161.9	0.08	1163.9	−0.08
8	1187.4	1234.4	−3.96	1187.3	0.01	1211.5	−2.03
9	1293.9	1292.4	0.11	1293.4	0.04	1297.8	−0.30
10	1325.8	1308.8	1.28	1325.1	0.05	1327.7	−0.14

Table 7
Natural frequencies of the discrete system for the texture 2 and scale factor $s = 1$.

Mode	1	2	3	4	5	6	7	8	9	10
Freq. [Hz]	146.1	387.4	426.0	775.8	976.6	1081.2	1176.2	1336.3	1437.0	1506.0

Table 8
Elastic constants for the texture 2 and scale factor $s = 1$.

Constants	Elastic constants		
	Homogenization	Static DE	Dynamic DE
A_{1111} [Pa]	125000000000	128261533654	248511143716
A_{2222} [Pa]	25000000000	24404348237	25472719233
A_{1212} [Pa]	10420000000	14110175388	15244814423
A_{2121} [Pa]	52080000000	21157038714	17890849722
D_{11} [Pa]	890000000	89000000	416908276
D_{22} [Pa]	170000000	226750433	233602617

the three different approaches are depicted in Fig. 9. All the models are capable to catch the mechanical behaviour of the discrete system. The MSEs are $5.60 \cdot 10^{-3}$ and $3.28 \cdot 10^{-4}$ for the homogenization and identification based on the static response, respectively. As in the previous case there is a decrease of the error as the internal size becomes smaller

The natural frequencies obtained for the different identifications are reported in Table 12. As for $s = 1$, a good accuracy is achieved and the identification based on the modal response is very precise for the higher frequency. The MSEs are $7.73 \cdot 10^{-2}$ and $1.32 \cdot 10^{-3}$ for the homogenization and modal-based identification, respectively. As for the

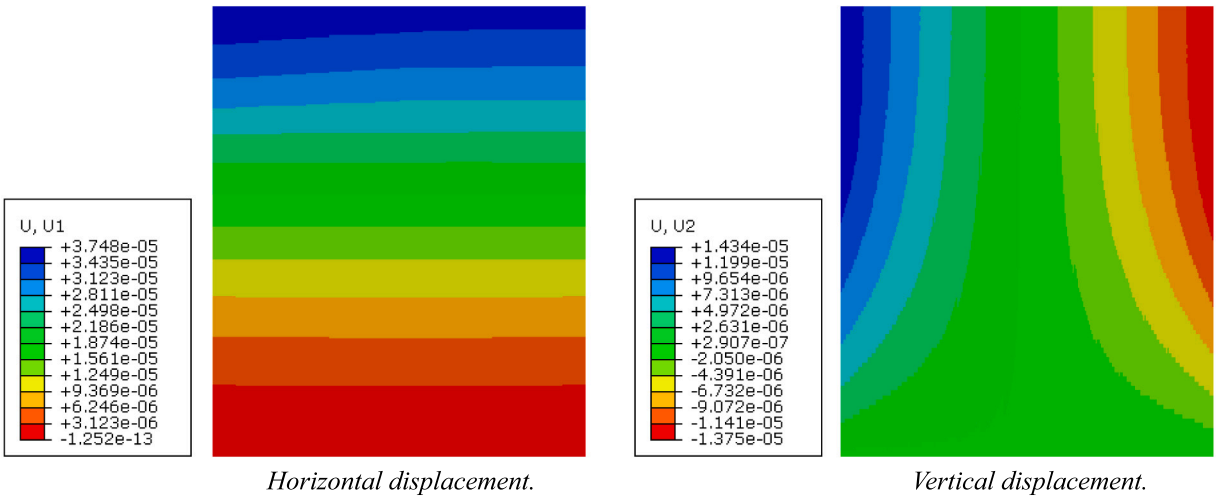

Fig. 8. Displacement fields of the Cosserat continua for the texture 2 with interlocking and scale factor $s = 0.5$.

Table 9
Natural frequencies for the texture 2 and scale factor $s = 1$.

Mode	Frequencies (Hz)						
	Discrete	Homogenization	Error [%]	Dynamic ID	Error [%]	Static ID	Error [%]
1	146.1	147.5	−0.93	147.45	−0.29	145.8	0.23
2	387.4	388.2	0.92	391.9	−0.03	383.6	2.09
3	426.0	426.2	−0.04	429.2	−0.74	425.0	0.23
4	775.8	789.3	−1.73	773.7	0.27	771.4	0.57
5	976.6	984.4	−0.80	979.5	−0.30	969.4	0.74
6	1081.2	1109.7	−2.63	1083.6	−0.23	1013.7	6.24
7	1176.2	1165.7	0.89	1176.6	−0.03	1151.7	2.08
8	1336.3	1335.8	0.04	1334.7	0.12	1315.3	1.57
9	1437.0	1472.9	−2.45	1435.9	0.07	1385.4	3.59
10	1506.0	1475.1	2.05	1504.3	0.11	1416.5	5.94

Table 10
Natural frequencies (Hz) of the discrete system for the texture 2 and scale factor $s = 0.5$.

Mode	1	2	3	4	5	6	7	8	9	10
Freq.	150.1	387.2	425.9	774.5	977.9	1074.8	1170.0	1334.9	1442.8	1510.9

Table 11
Elastic constants for the texture 2 and scale factor $s = 0.5$.

Constants	Elastic constants		
	Homogenization	Static DE	Dynamic DE
A_{1111} [Pa]	125000000000	125710477280	154354211117
A_{2222} [Pa]	25000000000	24928417128	25198537401
A_{1212} [Pa]	10420000000	13222253106	12433457509
A_{2121} [Pa]	52080000000	24669487148	28689073333
D_{11} [Pa]	220000000	22000000	22000000
D_{22} [Pa]	40000000	80000000	30484201

static case, a decrease of the internal scales leads to a decrease of the MSE for both approaches.

5. Conclusions

This work focuses on the derivation of the constituent terms of a micropolar continuum by exploiting the comparison between a discrete-continuous homogenization procedure (which dates back to the molecular theory of elasticity [6,54]), and an identification procedure based on structural optimization approach.

The obtained results show that the micropolar continuum provides a proper mechanical modelling for a composite material. Two different approaches for the estimation of the elastic constants of the micropolar have been illustrated. Both procedures can be considered reliable according to the high accuracy achieved in the computation of the displacement fields and natural frequencies with respect to the discrete reference model.

For both homogenization and identification approaches, the mean square errors of the objective functions return the lower values in the static case and the minimum error corresponds to the smallest scale, this is expected because in the case of materials with elements of small size, the dependence on the scale weakens.

The difference of the MSE between the homogenization and the identification procedures based on the DE algorithm are of 1 and 2 order of magnitude. The identification of the elastic constants via the optimization approaches provides satisfying results, however, to derive the elastic properties a benchmark solutions or direct tests on the material are necessary. Differently, for the homogenization procedure, only the detection of the representative volume element and the characteristics of the single constituents of the material are requested to derive the constitutive matrices.

The use of the DE for the identification of the micropolar constitutive constants appears to be a valid alternative to the homogenization procedure. This approach can be useful in the case of experimental tests, whereas significant measurements on the examined materials can be used to derive the elastic parameters of the material. Moreover, the same approach can be extended to derive the mechanical properties of other different materials.

A further extension of this study concerns the identification a nonlinear micropolar constitutive model (elasto-plastic model). In this

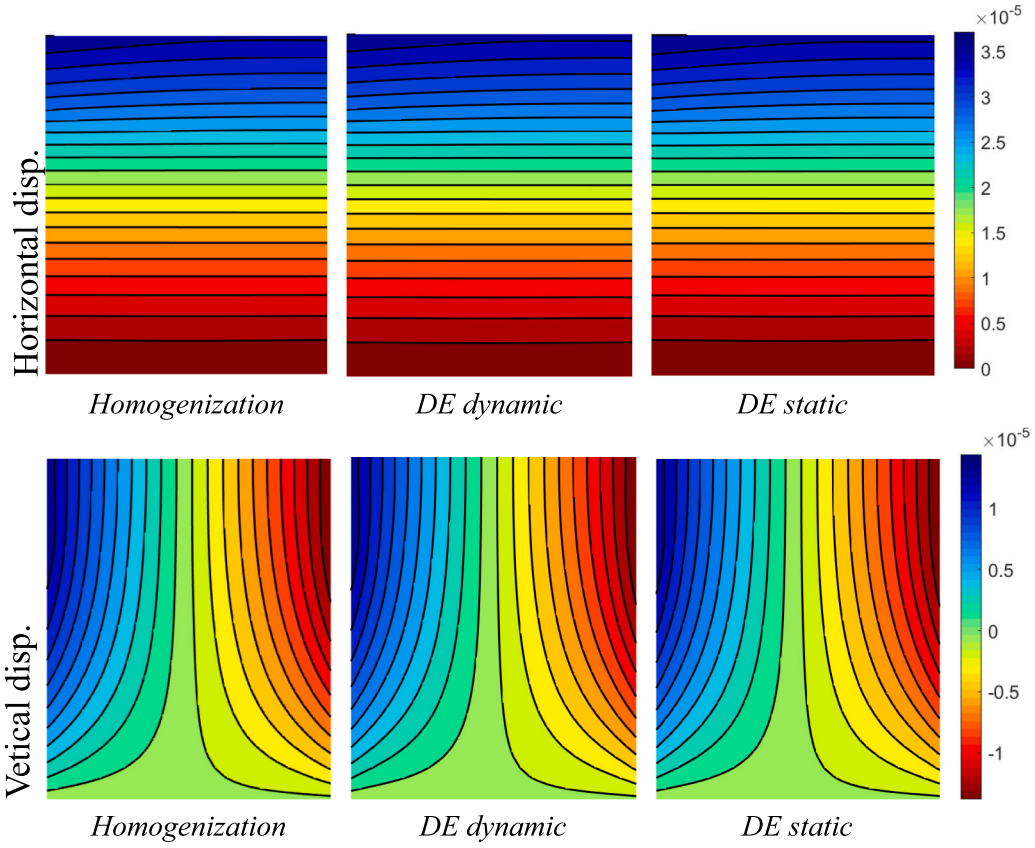

Fig. 9. Displacement fields of the Cosserat continua. Texture with no interlocking and scale factor $s = 0.5$.

Table 12
Natural frequencies for the texture 2 and scale factor $s = 0.5$.

Mode	Frequency (Hz)						
	Discrete	Homogenization	Error [%]	Dynamic ID	Error [%]	Static ID	Error [%]
1	150.1	146.1	2.70	145.8	2.85	145.8	2.84
2	387.2	388.2	−0.26	389.8	−0.68	387.7	−0.14
3	425.9	426.9	−0.23	426.3	−0.08	427.8	−0.45
4	774.5	780.6	−0.78	773.7	0.11	774.0	0.07
5	977.9	983.8	−0.60	978.5	−0.06	983.8	−0.60
6	1074.8	1105.6	−2.86	1076.2	−0.13	1062.7	1.12
7	1170.0	1165.7	0.36	1170.3	−0.02	1164.0	0.51
8	1334.9	1337.8	−0.21	1334.4	0.04	1332.6	0.17
9	1442.8	1467.4	−7.70	1443.2	−0.03	1453.4	−0.73
10	1510.9	1519.3	−0.55	1509.9	0.06	1495.2	1.04

framework, the identification procedure will be exploited for characterizing the parameters of the yield domains and their evolution (hardening/softening).

Declaration of competing interest

The authors declare that they have no known competing financial interests or personal relationships that could have appeared to influence the work reported in this paper.

Data availability

No data was used for the research described in the article.

Acknowledgements

This study is supported by: Italian Ministry of University and Research PRIN 2017, project No. 2017HFPKZY (B88D19001130001); Sapienza Research Grants, Italy "Progetti Grandi" 2018 (B81G19000060005).

References

[1] D. Baraldi, E. Reccia, A. Cecchi, In plane loaded masonry walls: DEM and FEM/DEM models. a critical review, Meccanica 53 (7) (2018) 1613–1628.

[2] P. Trovalusci, V. Varano, G. Rega, A generalized continuum formulation for composite microcracked materials and wave propagation in a bar, J. Appl. Mech. 77 (6) (2010).

[3] H. Reda, Y. Rahali, J.-F. Ganghoffer, H. Lakiss, Wave propagation in 3D viscoelastic auxetic and textile materials by homogenized continuum micropolar models, Compos. Struct. 141 (2016) 328–345.

[4] V. Settimi, P. Trovalusci, G. Rega, Dynamical properties of a composite microcracked bar based on a generalized continuum formulation, Contin. Mech. Thermodyn. 31 (6) (2019) 1627–1644.

[5] A.C. Eringen, Theory of micropolar elasticity, in: Microcontinuum Field Theories, Springer, 1999, pp. 101–248.

[6] P. Trovalusci, Molecular approaches for multifield continua: origins and current developments, in: Multiscale Modeling of Complex Materials, Springer, 2014, pp. 211–278.

[7] L. Leonetti, N. Fantuzzi, P. Trovalusci, F. Tornabene, Scale effects in orthotropic composite assemblies as micropolar continua: A comparison between weak-and strong-form finite element solutions, Materials 12 (5) (2019) 758.

[8] N. Fantuzzi, P. Trovalusci, R. Luciano, Multiscale analysis of anisotropic materials with hexagonal microstructure as micropolar continua, Int. J. Multiscale Comput. Eng. 18 (2) (2020).

[9] N. Fantuzzi, P. Trovalusci, R. Luciano, Material symmetries in homogenized hexagonal-shaped composites as cosserat continua, Symmetry 12 (3) (2020) 441.

[10] M. Colatosti, N. Fantuzzi, P. Trovalusci, R. Masiani, New insights on homogenization for hexagonal-shaped composites as cosserat continua, Meccanica (2021) 1–20.

[11] N. Fantuzzi, F. Shi, M. Colatosti, R. Luciano, Multiscale homogenization and analysis of anisotropic assemblies as cosserat continua, Int. J. Multiscale Comput. Eng. 20 (5) (2022) 87–103.

[12] M. Colatosti, F. Shi, N. Fantuzzi, P. Trovalusci, Mechanical characterization of composite materials with rectangular microstructure and voids, Arch. Appl. Mech. (2022).

[13] F. Shi, N. Fantuzzi, P. Trovalusci, Y. Li, Z. Wei, Stress field evaluation in orthotropic microstructured composites with holes as cosserat continuum, Materials 15 (2022) 6196.

[14] A. Pau, P. Trovalusci, Block masonry as equivalent micropolar continua: the role of relative rotations, Acta Mech. 223 (7) (2012) 1455–1471.

[15] P. Trovalusci, R. Masiani, Non-linear micropolar and classical continua for anisotropic discontinuous materials, Int. J. Solids Struct. 40 (5) (2003) 1281–1297.

[16] S. Brasile, R. Casciaro, G. Formica, Multilevel approach for brick masonry walls – part II: On the use of equivalent continua, Comput. Methods Appl. Mech. Engrg. 196 (49) (2007) 4801–4810.

[17] I. Stefanou, J. Sulem, I. Vardoulakis, Three-dimensional cosserat homogenization of masonry structures: Elasticity, Acta Geotech. 3 (1) (2008) 71–83.

[18] S. Brasile, R. Casciaro, Multilevel approach for brick masonry walls – part III: A strategy for free vibration analysis, Comput. Methods Appl. Mech. Engrg. 198 (49) (2009) 3934–3943.

[19] A. Bacigalupo, L. Gambarotta, Micro-polar and second order homogenization of periodic masonry, Mater. Sci. Forum 638–642 (2010).

[20] M.L. De Bellis, D. Addessi, A cosserat based multi-scale model for masonry structures, Int. J. Multiscale Comput. Eng. 9 (5) (2011).

[21] D. Addessi, A 2D cosserat finite element based on a damage-plastic model for brittle materials, Comput. Struct. 135 (2014) 20–31.

[22] M. Godio, I. Stefanou, K. Sab, J. Sulem, Dynamic finite element formulation for cosserat elastic plates, Internat. J. Numer. Methods Engrg. 101 (13) (2015) 992–1018.

[23] M. Godio, I. Stefanou, K. Sab, J. Sulem, Multisurface plasticity for cosserat materials: Plate element implementation and validation, Internat. J. Numer. Methods Engrg. 108 (5) (2016) 456–484.

[24] D. Baraldi, S. Bullo, A. Cecchi, Continuous and discrete strategies for the modal analysis of regular masonry, Int. J. Solids Struct. 84 (2016) 82–98.

[25] D. Baraldi, A. Cecchi, A. Tralli, Continuous and discrete models for masonry like material: A critical comparative study, Eur. J. Mech. A Solids 50 (2015) 39–58.

[26] M. Colatosti, N. Fantuzzi, P. Trovalusci, Time-history analysis of composite materials with rectangular microstructure under shear actions, Materials 14 (21) (2021).

[27] T. Sadowski, S. Samborski, Prediction of the mechanical behaviour of porous ceramics using mesomechanical modelling, Comput. Mater. Sci. 28 (3–4) (2003) 512–517.

[28] T. Sadowski, S. Samborski, Development of damage state in porous ceramics under compression, Comput. Mater. Sci. 43 (1) (2008) 75–81.

[29] H. Muhlhaus, Shear band analysis in granular material by cosserat theory, in: International Symposium on Numerical Models in Geomechanics, Vol. 2, 1986, pp. 115–122.

[30] M.T. Manzari, Application of micropolar plasticity to post failure analysis in geomechanics, Int. J. Numer. Anal. Methods Geomech. 28 (10) (2004) 1011–1032.

[31] K.A. Alshibli, M.I. Alsaleh, G.Z. Voyiadjis, Modelling strain localization in granular materials using micropolar theory: numerical implementation and verification, Int. J. Numer. Anal. Methods Geomech. 30 (15) (2006) 1525–1544.

[32] R. Dendievel, S. Forest, G. Canova, Estimation of overall properties of heterogeneous cosserat materials, 1998, http://dx.doi.org/10.1051/jp4:1998814, Vol. 8.

[33] S. Forest, K. Sab, Cosserat overall modeling of heterogeneous materials, Mech. Res. Commun. 25 (4) (1998) 449–454.

[34] S. Forest, F. Barbe, G. Cailletaud, Cosserat modelling of size effects in the mechanical behaviour of polycrystals and multi-phase materials, Int. J. Solids Struct. 37 (46) (2000) 7105–7126.

[35] D. Bigoni, W. Drugan, Analytical derivation of cosserat moduli via homogenization of heterogeneous elastic materials, 2007.

[36] A. Bacigalupo, L. Gambarotta, Second order computational homogenization of heterogeneous materials with periodic microstructure, ZAMM Z. Angew. Math. Mech 90 (2010) 796–811.

[37] L. Leonetti, F. Greco, P. Trovalusci, R. Luciano, R. Masiani, A multiscale damage analysis of periodic composites using a couple-stress/Cauchy multidomain model: Application to masonry structures, Composites B 141 (2018) 50–59.

[38] R. Luciano, J. Willis, Bounds on non-local effective relations for random composites loaded by configuration-dependent body force, J. Mech. Phys. Solids 48 (9) (2000) 1827–1849.

[39] R. Luciano, J. Willis, FE analysis of stress and strain fields in finite random composite bodies, J. Mech. Phys. Solids 53 (7) (2005) 1505–1522.

[40] M. Pingaro, E. Reccia, P. Trovalusci, R. Masiani, Fast statistical homogenization procedure (FSHP) for particle random composites using virtual element method, Comput. Mech. 64 (2019).

[41] A. Bacigalupo, L. Gambarotta, Non-local computational homogenization of periodic masonry, Int. J. Multiscale Comput. Eng. 9 (5) (2011).

[42] H. Altenbach, V.A. Eremeyev, Generalized Continua-from the Theory To Engineering Applications, Vol. 541, Springer, 2012.

[43] M. Colatosti, N. Fantuzzi, P. Trovalusci, Dynamic characterization of microstructured materials made of hexagonal-shape particles with elastic interfaces, Nanomaterials 11 (7) (2021) 1781.

[44] R. Storn, K. Price, Differential evolution–a simple and efficient heuristic for global optimization over continuous spaces, J. Global Optim. 11 (4) (1997) 341–359.

[45] M. Savoia, L. Vincenzi, Differential evolution algorithm for dynamic structural identification, J. Earthq. Eng. 12 (2008) 800–821.

[46] R. Greco, I. Vanzi, New few parameters differential evolution algorithm with application to structural identification, J. Traffic Transp. Eng. (Engl. Ed.) 6 (1) (2019) 1–14.

[47] E. Cevizci, S. Kutucu, M. Morales-Beltran, B. Ekici, M. Tasgetiren, Structural optimization for masonry shell design using multi-objective evolutionary algorithms: Present practices and future scopes, ISBN: 978-3-030-01640-1, 2019, pp. 85–119.

[48] M. Babaei, M. Mollayi, An improved constrained differential evolution for optimal design of steel frames with discrete variables, Mech. Based Des. Struct. Mach. 48 (6) (2020) 697–723.

[49] G. Quaranta, G. Marano, R. Greco, G. Monti, Parametric identification of seismic isolators using differential evolution and particle swarm optimization, Appl. Soft Comput. 22 (2014) 458–464.

[50] H. Tang, S. Xue, C. Fan, Differential evolution strategy for structural system identification, Comput. Struct. 86 (21) (2008) 2004–2012.

[51] S. Casciati, Stiffness identification and damage localization via differential evolution algorithms, Struct. Control Health Monit. 15 (3) (2008) 436–449.

[52] S. Seyedpoor, S. Shahbandeh, O. Yazdanpanah, An efficient method for structural damage detection using a differential evolution algorithm-based optimisation approach, Civ. Eng. Environ. Syst. 32 (3) (2015) 230–250.

[53] B. Carboni, A. Arena, W. Lacarbonara, Nonlinear vibration absorbers for ropeway roller batteries control, Proc. Inst. Mech. Eng. C 235 (20) (2021) 4704–4718.

[54] P. Trovalusci, R. Masiani, Material symmetries of micropolar continua equivalent to lattices, Int. J. Solids Struct. 36 (14) (1999) 2091–2108.

[55] M. Godio, I. Stefanou, K. Sab, Effects of the dilatancy of joints and of the size of the building blocks on the mechanical behavior of masonry structures, Meccanica 53 (7) (2017) 1629–1643.

[56] F. Shi, N. Fantuzzi, P. Trovalusci, Y. Li, Z. Wei, The effects of dilatancy in composite assemblies as micropolar continua, Compos. Struct. 276 (2021) 114500.

[57] R. Masiani, N. Rizzi, P. Trovalusci, Masonry as structured continuum, Meccanica 30 (6) (1995) 673–683.

[58] P. Trovalusci, G. Augusti, A continuum model with microstructure for materials with flaws and inclusions, Le J. de Phys. IV 8 (PR8) (1998) Pr8–383.

[59] B. Carboni, W. Lacarbonara, Nonlinear vibration absorber with pinched hysteresis: theory and experiments, J. Eng. Mech. 142 (5) (2016) 04016023.

[60] A. Ferreira, N. Fantuzzi, MATLAB Codes for Finite Element Analysis 2nd edition: Solids and Structures, Springer, New York, 2020.